A&A 384, 620–628 (2002)
DOI: 10.1051/0004-6361:20020009

Astronomy & Astrophysics

Turbulent planetary nebulae around [WC]–type stars⋆

A. Acker[1], K. Gesicki[2], Y. Grosdidier[3], and S. Durand[4]

[1] Observatoire astronomique de Strasbourg, 11 rue de l'Université, 67000 Strasbourg, France
[2] Centrum Astronomii UMK, ul.Gagarina 11, 87-100 Torun, Poland
e-mail: Krzysztof.Gesicki@astri.uni.torun.pl
[3] Instituto de Astrofísica de Canarias, C/. Vía Láctea s/n, 38 200 La Laguna (Tenerife), Spain
e-mail: yves@ll.iac.es
[4] Instituto astronomico e geofísico da USP, Av. Miguel Stefano 4200, 04301-904, São Paulo SP, Brazil
e-mail: durand@iagusp.usp.br

Received 19 July 2001 / Accepted 19 December 2001

Abstract. Through a high-resolution spectroscopic survey, we analyze the velocity field of 16 planetary nebulae with [WC]- or *wels*-type nuclei in comparison with 8 nebulae having other central star types. We found spectral evidence for finite turbulent velocities in [WC]-type planetary nebulae superimposed on an essentially constant expansion velocity pattern. The nebulae around O-type stars show no evidences for significant turbulence while their expansion velocity is found to increase outwards. Both types of nebulae show the same mean expansion velocity. Our results support the earlier suggestions that nebulae surrounding [WC] central stars are likely related to long-lasting momentum-driven phase bubbles. Turbulence in the nebulae can be either triggered, or enhanced, by stellar wind inhomogeneities that appear ubiquitous in Wolf-Rayet nuclei.

Key words. planetary nebulae: general – stars: Wolf–Rayet – turbulence

1. Introduction

Planetary nebulae (PN) morphologies are well explained in the framework of the interacting stellar wind model (see Kwok et al. 1978; Balick 1994). The resultant shells are subject to instabilities related to shocks and unstable ionization fronts, leading to a fragmentation of matter. Thus, fine nebular structure could be related to supersonic turbulence in the interaction zone, with additional structures possibly arising from clumping of the stellar winds.

Little quantitative information is available as yet on the suspected turbulent velocities. When observed at high spatial resolution (HST, ESO/NTT and VLT images), PN exhibit small-scale inhomogeneities not taken into account in current interacting stellar wind models. Simplified models have only considered white noise in the spatial distribution of velocity and density.

Recall recent spectroscopic data, obtained by Grosdidier et al. (2000, 2001a) and Acker & Grosdidier (2001), showing that turbulent-like outflows are systematically detected in the winds of [WC]-type nuclei of PN. These studies suggest that wind clumping potentially affect *all* [WC] central stars and the question arises as to the impact of wind inhomogeneities on nebular dynamics.

The aim of this paper is to compare the velocity field of PN with and without a [WC]-type nucleus and show how the nebular properties could be changed by the presence of a [WC] central star. Many publications have been devoted to [WC]-type stars and to their surrounding nebulae. Zijlstra (2001) reported on infrared observations, and found some unique double chemistry exclusively present within a subgroup of [WC] PN. Szczerba et al. (2001) reported a much higher percentage of PAH features among [WC] PN than in other nebulae.

However, on the whole it seems that planetary nebulae around [WC] nuclei have similar properties compared to other galactic PN, all PN having the same galactic distribution, morphologies, as well as similar chemical abundances. The only significant difference between the two groups of PN may be the amplitudes of the expansion velocities (see Acker et al. 1996; Górny 2001).

Concerning the velocity field, in our earlier paper (Gesicki & Acker 1996) we found that the nebulae around three [WC] stars show highly broadened profiles for three nebular lines, namely [O III] 5007 Å, [N II] 6584 Å and Hα (see Fig. 1). This implies the existence of turbulent motions or strong variations of the expansion in the radial direction relative to the central core.

Send offprint requests to: A. Acker,
e-mail: acker@astro.u-strasbg.fr

⋆ Based on observations obtained at the European Southern Observatory and the Observatoire de Haute Provence.

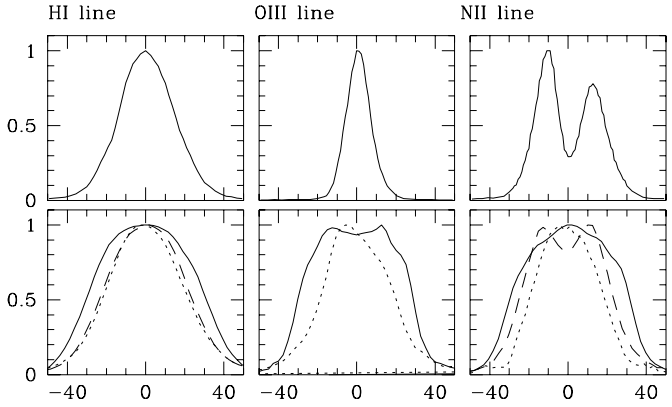

Fig. 1. Comparison between spectral lines of PN G 215.2-24.2 (IC 418) (upper boxes) and three PN with [WC] central stars (lower boxes, PN G 4.9+4.9 (M 1-25) –solid line, PN G 6.8+4.1 (M 3-15)–dotted line, PN G 285.4+1.5 (Pe 1-1)–dashed line). The figure is taken from Gesicki & Acker (1996).

Since 1994, we performed a spectroscopic survey to verify these conclusions on a larger sample of high resolution spectra. In Sect. 2 of the present paper, we present the observations of 16 newly observed PN and the modelling of 9 of them. In Sect. 3 we compare the velocity field of a large sample of PN with emission-lines nuclei as well as with other types of central stars. In Sect. 4 we discuss a possible connection between turbulent stellar winds and turbulent nebulae.

2. The observations of 16 PN and the analysis

2.1. The observations

In June 1997 and June 1998, we observed 16 PN with the ESO 1.4 m CAT telescope, equipped with the Coude Echelle Spectrometer (CES). The Hα-6562 Å and [N II]-6584 Å lines were observed with a resolving power of 50 000 in 1997 (f/4.7 Long Camera) and 70 000 in 1998 (f/12.5 Very Long Camera) used for PN G 001.5-06.7, 027.6+04.2, 352.9+11.4, and 359.2-33.5. The effective integration times varied from 1 hour (PN G 001.5-06.7) to 5 hours.

All the spectra were reduced in the usual way by using the MIDAS package, including bias subtraction, flat field correction, and wavelength calibration.

Some nebulae are large and resolved along the long slit, while others are unresolved. Therefore we decided to extract the central part of the spectra, corresponding to approximately a $2'' \times 2''$ area on the sky. This extraction was applied to all 16 spectra.

Seven of the observed objects were not suitable for our model analysis, as they show complicated structures in their spectra (and sometimes in the images). These observations are shown in Fig. 2. The top three objects have a [WC]-type nucleus.

The nebula PN G 002.4+05.8 ([WC4]), is very large, and the spectrum appears irregular along the slit. For PN G 332.9-09.9 ([WC11]) the nebular spectrum is

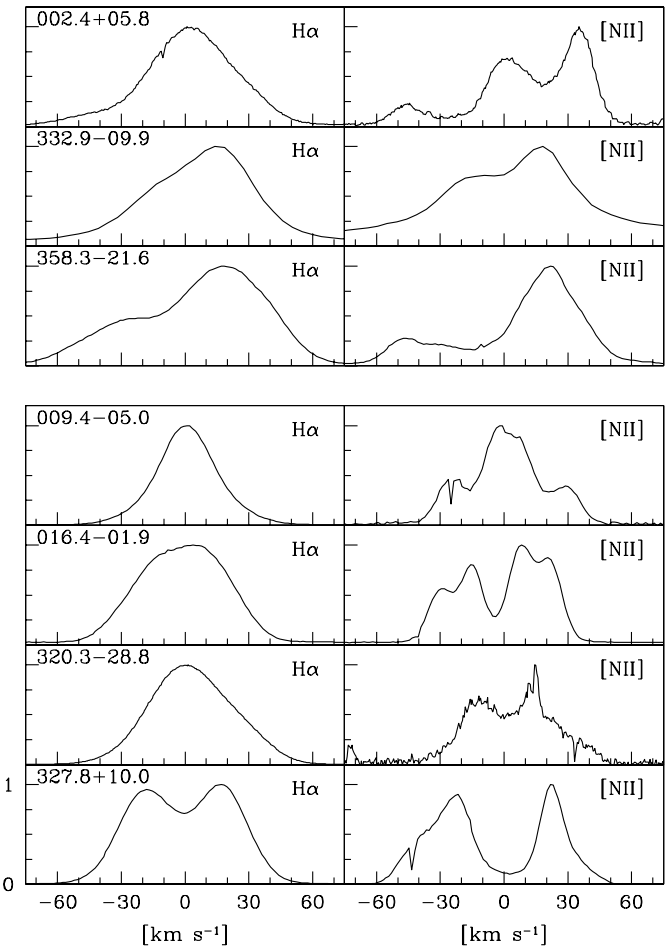

Fig. 2. Observed lines of Hα and [N II] 6584 Å. Three PN with [WC] nuclei, PN G 2.4+5.8 (NGC 6369, [WC4]), PN G 332.9-9.9 (He 3-1333, [WC11]), PN G 358.3-21.6 (IC 1297, [WC3]) are separated from the others: PN G 09.4-5.0 (NGC 6629), PN G 16.4-1.9 (M 1-46), PN G 320.3-28.8 (He 2-434) and PN G 327.8+10.0 (NGC 5882). The scale is given in the lowest boxes. These 7 objects are not suitable for modelling and were excluded from the final sample.

severely contaminated by the spectrum of the central star, especially by strong C II red lines. Note that the HST image obtained by de Marco et al. (1997) reveals a highly complex structure. For PN G 358.3-21.6 ([WC3]) the long slit spectrum reveals complex structures with many components of different velocities.

Four not-modelled PN have a nucleus without emission-lines. PN G 009.4-05.0 is a large nebula characterized by a faint surface brightness, the [N II] line being very weak. For PN G 016.4-01.9, PN G 320.3-28.8 and PN G 327.8+10.0 the long-slit spectra reveal bipolar or irregular structure in all cases.

Nine PN with fairly symmetric line profiles can be modelled (see Fig. 3), and are listed in Table 1.

Table 1. The comparison between the models and the observational data.

PN G	name	log $F(\mathrm{H}\beta)$ dereddened		electron temp. [10^4 K]		electron dens. [10^3 cm^{-3}]		line intensities rel. to $I(\mathrm{H}\beta) = 100$ [O III] 5007 Å		[N II] 6584 Å		[S II] 6731 Å	
		obs.	mod.	T[O III]	mod.	N[S II]	mod.	obs.	mod.	obs.	mod.	obs.	mod.
001.5-06.7	SwSt 1	−9.11	−9.1	1.06	1.0	280	360	33	30	59	12	0.7	0.4
003.1+02.9	Hb 4	−10.25	−10.15	0.96	0.9	4.6	7	1260	1500	91	84	7	3
027.6+04.2	M 2-43	−10.3	−10.3	1.05	1.1	10.1	43	519	630	133	58	2:	2
029.2-05.9	NGC 6751	−11.0	−10.3	1.12	0.95	2.73	2.0	1240	760	143	170	9	7
327.1-02.2	He 2-142	−10.9	−10.5	0.71	0.65	43.73	13	6	2	384	290	7	10
345.2-08.8	Tc 1	−10.4	−10.3	0.81	0.85	1.81	4.1	102	175	105	66	3	0.04
352.9+11.4	K 2-16	−12.2	−12.3	1.17	0.83	0.5	0.3	117	68	206	15	25	1
355.9-04.2	M 1-30	−10.77	−10.7	0.67	0.71	5.84	6.4	144	147	309	259	7	7
359.2-33.5	CRBB 1	-	−10.3	-	0.7	4	3.3	-	7	234	264	-	12

2.2. The computer codes

The computer codes for calculating the photo-ionization structure and emission line profiles are described in details in Gesicki et al. (1996) and summarized in our later papers on analysis of nebular line shapes. Here we repeat a brief description.

A photo-ionization model was constructed for each object. The nebula is approximated by a spherical shell defined by an inner and an outer radius, a total mass and a radial density distribution. The central star is approximated by a black-body atmosphere defined through the effective temperature and the luminosity.

Subsequently, a radial velocity profile is assumed, with the velocity varying smoothly with radius. The predicted profile for the emission line is calculated by integrating the velocity field over the ionization equilibrium and resulting line emission coefficients. The slit parameters and seeing are used as input parameters for this calculation. Comparing the predicted profile with the observations allows one to correct the assumed velocity field.

2.3. Modelling the 9 nebulae

The photo-ionization model requires the knowledge of stellar and nebular properties as initial parameters. They are taken from the literature and presented in Table 1. These values are often slightly changed during the fitting procedure in order to reproduce the observed Hβ flux and the line ratios (taken from the SECGPN, Acker et al. 1992). The adopted nebular and stellar parameters are presented in Table 2 (see the next section), where the nebulae studied in this survey are marked with an asterisk (*).

The photo-ionization model also requires the nebular abundances. As described in Gesicki et al. (1996) we applied an average nebular chemical composition, but whenever possible we supplemented the data by the values found in the literature, in particular the values published in Koeppen et al. (1991) and Peña et al. (2001).

For many objects, monochromatic images were published, which helped to establish the density profile inside the nebula. Unfortunately they are often not detailed enough, and in most cases they provide only approximate sizes for the inner nebular radius. For the hardest cases we fixed the inner radius to be about 0.4 of the outer one. For all objects, we assumed an inverted parabolic shape density distribution with the central density being twice as large as the density on the edge.

Our model is assumed to be ionization bounded, i.e. the outer radius is expected to correspond to the ionization boundary. Within such a model the line ratios are usually well reproduced, especially those formed in the outer regions. However, in three cases discussed below, we assumed a density bounded shell.

Distance is a crucial parameter for the determination of stellar and nebular parameters. In all cases we adopted a distance (given in Table 2) consistent with the best photo-ionization model, in agreement with published electron densities (given in Table 1). Assuming larger distances should result in larger and less dense nebulae. Assuming smaller distances should result in smaller radii and therefore higher densities. The adopted stellar luminosity (Table 2) is calculated in order to ionize enough mass to reproduce the observed $F(\mathrm{H}\beta)$ flux (Table 1).

2.4. Deriving the expansion velocities

Because of inherent simplifications of the model and observational limitations due to the spectral resolution and variable seeing, we always searched for the simplest velocity fields. Whenever possible, we assumed a constant velocity pattern. Whether there was an indication of acceleration, we used a smoothly increasing velocity. When a simple velocity field was not found to reproduce the line shapes, we introduced a turbulent broadening.

The observed profiles (circles) together with the model best fitted profiles (solid curves) are presented in Fig. 3.

The derived expansion velocities are presented in Table 2, in the last three columns with the common header "results". The column v_{exp} contains the value of a constant velocity field, or in case of acceleration (i.e. when $\Delta v > 0$) the mass weighted average velocity (see Gesicki et al. 1998). The difference between velocities at the outer and inner radius is given in next column: Δv. In the

Table 2. The stellar and nebular parameters applied for the modelling and the resulting expansion velocities. The data from the present survey are marked with an asterisk *. For two objects we present two velocity solutions. The entries are grouped according to the central star type.

PN G	name	central star			dist.	$c(\mathrm{H}\beta)$	planetary nebula			results		
		spect. type	$T_{\rm eff}$ [kK]	$\log(L)$ $[L_\odot]$	[kpc]		diam $''$	$R_{\rm out}$ [pc]	$M_{\rm ion}$ $[M_\odot]$	$v_{\rm exp}$	Δv	$v_{\rm turb}$
										[km s^{-1}]		
003.1+02.9 *	Hb 4	WC 3	90	3.6	4	1.7	6.7	0.065	0.2	16	0	14
029.2-05.9 *	NGC 6751	WC 4	80	3.0	2	0.7	21	0.1	0.15	41	0	15
144.5+06.5	NGC 1501	WC 4	141	3.8	1.2	1.2	55	0.16	0.18	40	0	10
285.4+01.5	Pe 1-1	WC 4–5	85	3.3	3.5	1.87	3	0.05	0.038	24	0	10
006.8+04.1	M 3-15	WC 4–6	79	3.6	4	2.1	5	0.06	0.19	16	0	15
004.9+04.9	M 1-25	WC 6	42	3.8	8	1.4	3.2	0.06	0.18	30	0	12
120.0+09.8	NGC 40	WC 8	33	3.3	1.2	0.52	47	0.14	0.25	25	0	8
027.6+04.2 *	M 2-43	WC 8	65	3.6	5	2.8	1.6	0.02	0.04	20	0	10
327.1-02.2 *	He 2-142	WC 9	26	3.7	3.5	1.3	3.6	0.03	0.03	20	0	7
										21	20	0
064.7+05.0	BD +30 3639	WC 9	26	4.1	2.6	0.36	5.6	0.035	0.08	27	0	15
146.7+07.6	M 4-18	WC 11	25	3.8	6.8	0.9	3.6	0.06	0.1	15	0	15
352.9+11.4 *	K 2-16	WC 11	29	3.3	1	0.25	20	0.05	0.002	34	0	12
										38	35	0
001.5-06.7 *	SwSt 1	wels	33	4.3	2	1.22	1.3	0.007	0.01	17	12	14
096.4+29.9	NGC 6543	wels	50	3.6	1.12	0.03	18	0.05	0.12	17	0	12
355.9-04.2 *	M 1-30	wels	40	3.8	8	1	3.6	0.07	0.22	22	28	0
221.3-12.3	IC 2165	wels	155	3.2	2.5	0.5	7.8	0.057	0.076	25	15	14
008.3-01.1	M 1-40	cont	140	3.3	2.5	2.7	4.6	0.042	0.067	27	20	0
005.8-06.1	NGC 6620	cont	110	3.3	8	0.6	6	0.14	0.45	27	25	0
005.2+05.6	M 3-12	cont	100	3.2	8	1.1	6.5	0.15	0.57	30	20	0
261.0+32.0	NGC 3242	O(H)	79	3.3	1	0.09	41	0.1	0.15	31	35	0
123.6+34.5	IC 3568	O3(H)	48	3.9	2	0.4	20	0.1	0.13	29	35	0
215.2-24.2	IC 418	Of(H)	37	3.9	1	0.05	14	0.036	0.05	15	22	0
345.2-08.8 *	Tc 1	Of(H)	32	3.5	2	0.3	10	0.05	0.05	20	34	0
359.2-33.5 *	CRBB 1	O(H)	27	3.8	3.5	-	9	0.08	0.18	13	21	0

column $v_{\rm turb}$ we give the derived value for the turbulent broadening.

For two objects we found, as described below, two equally good fits of line profiles with quite different velocity fields. For PN G 327.1-02.2, the [N II] line does not show the same Gaussian shape as the hydrogen line. The PN G 352.9+11.4 spectrum is under-exposed therefore noisy. In both cases an acceleration can mimic the turbulent broadening. The two possibilities are included in the Table 2, but for further discussion and graphic presentations we only considered the turbulent solutions. Both nebulae are built as a relatively thin shell with a relatively large inner radius.

The spectral type of the nuclei (Col. 3) are taken from Acker et al. (1992), and include the *wels*-type, for "weak-emission-line stars" defined in Tylenda et al. (1993). We attribute a "cont" type to stellar spectra without emission nor absorption pattern.

Except for one PN, our results are based on two spectral lines only. The [N II] lines originate in the outer nebular regions, whereas the hydrogen lines, formed throughout the whole nebula, are severely thermally broadened and smear the details of the velocity field. Therefore we can expect that the expansion velocities obtained in Sect. 2 are more relevant to the outer region. For a constant velocity expansion this has no influence but in the case of acceleration, the obtained velocities could be biased towards larger values.

Simultaneous fits of more spectral lines, covering the whole nebulae, would allow more reliable velocity field derivations, in particular for the two mentioned above ambiguous cases.

2.5. Comments on individual nebulae

PN G 001.5-06.7 This is the only object for which the observations are supplemented by the [O III]-5008 Å line taken from Gesicki & Zijlstra (2000). Therefore the results of the modelling are more reliable than for the other nebulae. The *FWHM* of the [O III] 5007 Å line is about 5 km s^{-1} smaller than that of [N II] 6584 Å. This indicates a moderate acceleration. However the three lines reveal broad Gaussian wings suggesting a rather strong turbulence. The derived velocity field is therefore linearly increasing with additional turbulent broadening.

PN G 003.1+02.9 The spectral lines are not symmetric. The red wings of the lines can be best fitted with

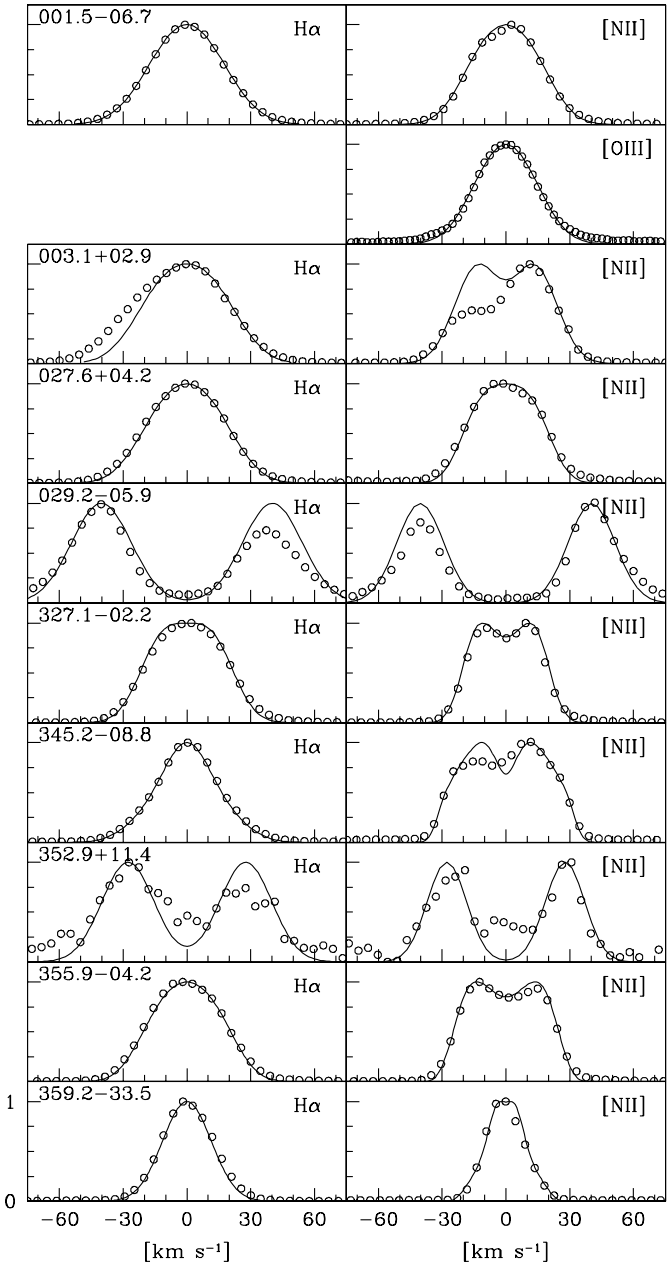

Fig. 3. Observed and modelled lines of Hα and [N II] 6584 Å and for one case the [O III] 5007 Å. The circles correspond to the observations, the solid curves to the calculated model. The intensities are normalized to unity, the scale is given in the lowest boxes

Gaussian-like strongly broadened functions. The left part of the Hα profile shows a bump clearly not Gaussian and we interpret it as a higher velocity blob which happened to appear within the spectrograph slit.

PN G 027.6+04.2 Despite reducing the inner radius the model remains still too dense as compared with observations (see Table 1).

PN G 029.2-05.9 The image of Schwarz et al. (1992) as well as our long slit spectra indicate a relatively large inner radius. For this PN we adopted a density bounded model, because the central star can ionize much more mass than is needed to reproduce the observed flux in Hβ. Nevertheless we see that the line ratios are well reproduced. A constant expansion velocity with turbulence reproduces well the line shapes observed in the small central area of this large nebula.

PN G 327.1-02.2 The HST image (Sahai & Trauger 1998) suggests that we should consider a relatively thin shell with a large inner radius. The modelled line shapes assume constant velocity plus small turbulence, but we must admit that an equally good fit could be achieved without additional turbulence but with the velocity linearly increasing from 10 to 30 km s^{-1}. Both solutions are presented in Table 2.

PN G 345.2-08.8 For this PN we adopted a density bounded model, because the central star can ionize much more mass than is needed to reproduce the observed flux in Hβ. The image of Schwarz et al. (1992) shows no central cavity, so we assumed a very small inner radius. The velocity field which steeply increases in the outer layers reproduces surprisingly well the line shapes which are very different for both ions.

PN G 352.9+11.4 The image of Schwarz et al. (1992) and our long slit spectra indicate a very large inner radius. The presented model is density bounded, otherwise the flux F(Hβ) would become much larger than observed. The spectrum of this big and weak nebula is very noisy. As for NGC 6751, two solutions presented in Table 2 are acceptable.

PN G 355.9-04.2 For this PN we assumed the Galactic Bulge distance, which allows one to build a good photoionization model. The *FWHM* of the [N II] 6584 Å line is about 8 km s^{-1} broader than that of Hα. This clearly suggests a velocity gradient in the nebula. The presented fit is obtained without any additional turbulence.

PN G 359.2-33.5 The image by McCarthy et al. (1991) shows no ring features. An increasing velocity without turbulence is deduced for this object.

For the 7 PN with asymmetric and complicated line profiles (shown in Fig. 2), no modelling was performed. The line profiles of the 4 non-[WC] nuclei don't support the assumption of turbulent velocities. For the three PN with [WC] nuclei (PN G 2.4+5.8 NGC 6369, [WC4]; PN G 332.9-9.9 He 3-1333, [WC11]; PN G 358.3-21.6 IC 1297, [WC3]), the profiles appear broadened for the 2 observed lines, implying possible turbulent motions.

3. Are expansion and/or turbulent motions correlated with stellar parameters?

In a series of papers we already have analyzed the velocity fields in a number of nebulae with [WC]-type central stars and with O-type nuclei. The analyzed PN were observed from 1993 to 1998 at high resolution ($R = 50\,000$ to 70 000) with the ESO 1.4 m CAT telescope, and the OHP 1.5 m and 1.9 m telescopes. In Table 2 we assembled the data from Gesicki & Acker (1996), Gesicki et al. (1996, 1998), Neiner et al. (2000) together with the data from the present survey. For IC 2165, our spectrum shows some

indication of stellar emissions, allowing us to classify the nucleus as being of *wels*-type.

Note that the whole sample presented in Table 2 is selected in the same way and analyzed using the same computer code, although published over years.

The statistical significance of the final sample should be discussed. In our earlier paper (Gesicki et al. 1998), we analyzed the correlation found between the presence of an ionization front and the acceleration in the outer layers of the nebulae. We speculated that when the ionization front approaches the nebular edge, it accelerates the outer layers and it is what we observe. When the ionization front breaks through the outer layers, the PN looses sphericity and symmetry in line profiles, and we reject it from our sample.

Now, we may revise this discussion. We found one object (PN G 345.2-08.8) which is density bounded, i.e. without an ionization front but with accelerated outer layers. Additional doubts come from many [WC]-type PN which are not accelerated (however turbulent) but are ionization bounded.

Only five of our objects are density bounded: three [WC]-type and two of type O. Note that all three density bounded [WC]-type nebulae have also the fastest expansions.

Despite the doubts, it still seems that our selection criterion prefers the ionization bounded nebulae (19 from 24). In this case we see the ionization sphere expanding into the ambient neutral gas so the symmetry is natural. Searching for other dependencies was not successful because the Table 2 presenting the nebular parameters shows large scatter in the values. For instance, we cannot state that the ionization bounded nebulae are more massive or smaller than the other.

3.1. The expansion velocity

The 3 groups of PN according to the type of their central star (see Table 2) show about the same mean value of the expansion velocity. The mean expansion velocity obtained for the [WC] group is 26 $\mathrm{km\,s^{-1}}$, 20 $\mathrm{km\,s^{-1}}$ for the *wels*-group, and 24 $\mathrm{km\,s^{-1}}$ for the other PN, while the median values are: 25, 20 and 27 respectively. The statistics is based on a limited sample, nevertheless we can conclude that the mean expansion velocities for [WC]-type nebulae are not significantly different from those of "normal" PN – except for the [WC4]-PN NGC 6751 and NGC 1501 which show faster expansion. The four PN with *wels* nuclei seem to expand slower.

Now we can prove on a larger and uniform sample, that for all PN with [WC]-type nuclei the internal motions are best represented by a constant expansion velocity with superimposed (presumably supersonic) turbulence. On the contrary the non-[WC] PN show no sign of such high turbulence but they present clear evidence for outward acceleration. There are two [WC]-type PN for which alternative non-turbulent velocity solutions exist, but there are

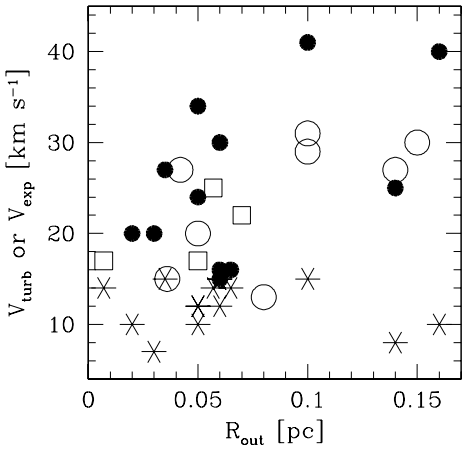

Fig. 4. Nebular radius vs. expansion and turbulent velocity. Expansion velocities are coded: black circles – [WC], open squares – *wels*, open circles – other nuclei types. Turbulent velocities are coded by asterisks.

no turbulent solutions for non-[WC] nebulae. However the *wels* (or suspected *wels*) nuclei don't follow this simple classification scheme.

Our mean values of expansion velocity for non-[WC] nebulae is higher than the value of 21 $\mathrm{km\,s^{-1}}$ obtained by Gesicki & Zijlstra (2000). This difference can be easily explained because their value was obtained from the [O III] 5007 Å line which is probing the inner and slower expanding nebular regions. Górny & Stasińska (1995) analyzing compilations of data found that on average the PN with [WC]-type nuclei expand faster than other PN. Their mean values are 30.9 and 19.4 $\mathrm{km\,s^{-1}}$ for each class respectively, while our data show rather no difference. The discrepancy should be explained as follows. At low spectral resolution, the structure of the line profiles is not visible, and the broadening of line profiles (due in fact to both expansion and turbulent velocities) were interpreted as uniquely due to high expansion velocities.

A weak correlation appears between nebular radius and expansion velocities (Fig. 4): larger PN seem to expand faster than small PN, as also pointed out by Gesicki & Zijlstra (2000). Note also that the smallest values of the turbulent velocity correspond to larger radii (>0.1 pc), density bounded nebulae.

3.2. The stellar parameters

We present in Fig. 5 the obtained expansion and turbulent velocities versus the classification of the [WC]-nuclei. No correlation appears, as found by others authors (e.g. expansion velocities by Peña et al. 2001).

For all types of PN, no correlation was found between the velocities and the nuclei temperature, nor the stellar luminosity (see the HR diagram in Fig. 6).

The dynamical ages of the PNe can be calculated from the ratio of the nebular radius over the expansion velocity. No correlations have been found except of obvious

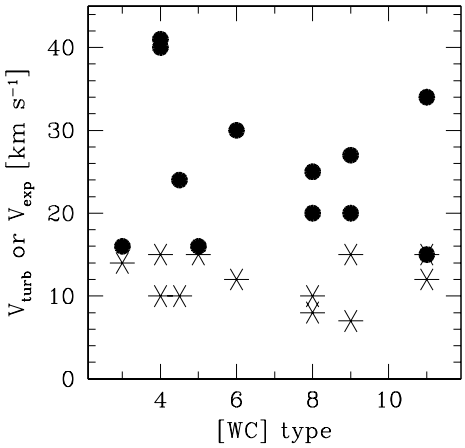

Fig. 5. Expansion (dots) and turbulent (asterisks) velocities plotted against the [WC] type.

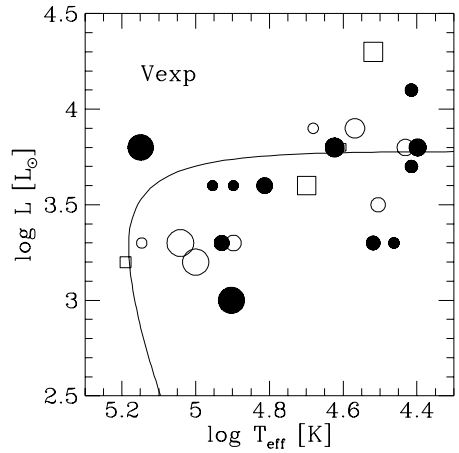

Fig. 6. H-R diagram for PN nuclei: black circles – [WC], open squares – *wels*, open circles – other. The size of the symbols is proportional to the expansion velocity. The evolutionary track is from Bloecker (1995).

dependencies that the older nebulae are larger and more massive.

From the dynamical ages and stellar temperatures the central star masses can be estimated (Gesicki & Zijlstra 2000). This method applies evolutionary tracks. The evolutionary paths of [WC]-type central stars are still debated, however there are some evidences that they cannot be much different from those of normal PN cores (Górny 2001). We estimated the core masses for all objects of our sample, the search for correlations failed also in this case. What can be stated here is that the [WC]-type nuclei do not differ from other PN nuclei with respect to stellar masses.

Finally, we used the C III and C IV stellar lines profiles to derive the terminal velocity of the [WC] wind proportional to the *FWHM* of the lines (see Acker & Durand 2001). No correlation is found between the terminal velocity and nebular expansion or turbulence. But, as shown in Fig. 7, a clear dependence was found between terminal velocity and the ionized mass, and also the dynamical age

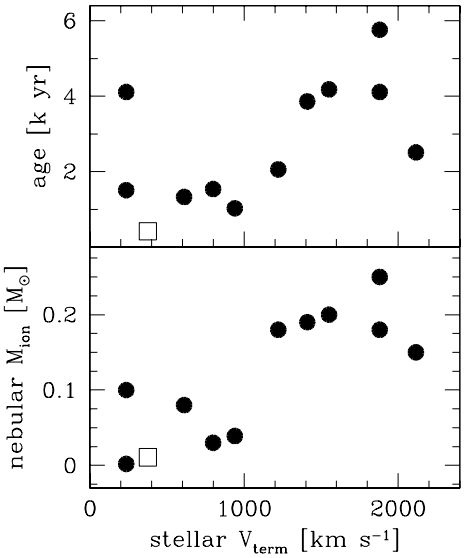

Fig. 7. Terminal velocity of the stellar wind versus the nebular dynamical age (upper box) and the ionized mass of the PN (lower box).

of the nebula. From this dependence we can expect that it is possible to follow the mass-loss history for [WC]-type nuclei.

4. The origin of turbulence

Different questions arise: are turbulent velocities inside the nebulae around [WC]-type nuclei linked with the apparently universal stellar wind fragmentation in [WC] stars (Grosdidier et al. 2000, 2001a; Acker & Grosdidier 2001)? Is the mass-loss history of [WC] nuclei different from those of other central stars of PN?

It is worth noting that as the central star evolves through the post-AGB phase, the density of the fast wind decreases, while its terminal velocity increases. The very strong dependence of the cooling time with the terminal velocity thus makes the radiative cooling of the shocked fast wind less and less efficient. Therefore, PN are expected to be initially momentum-driven and later to become energy-driven, the transition occurring for a critical terminal velocity of about $v_c = 150$ km s^{-1} (Kahn & Breitschwerdt 1990).

During the energy-driven phase, stellar wind inhomogeneities should be rapidly smoothed out by pressure waves in the hot bubble, they generally cannot be persistent enough to reach nebular distances. The link between fragmented winds and turbulent nebulae is very difficult to assess. Indeed, the most dense wind inhomogeneities, which are expected to last longer, cannot reach nebular distances easily (for a tentative approach see Grosdidier et al. 1999). The persistence of stellar wind inhomogeneities seems to strongly depend on at least i) the density contrast (about 50 or even more) between any individual wind clump and the mean, homogeneous, underlying ambient wind, in conjunction with

ii) photoionization shield effects (e.g. Mellema et al. 1998; Grosdidier et al. 1999) and/or iii) countervailing temperature contrasts (Owocki et al. 2000).

This makes the connection between the star and the nebula very difficult to prove observationally in most cases (e.g. Grosdidier et al. 2001b), the massive WR nebula RCW 104 possibly showing the best example of stellar clumps detected at nebular distances (Goudis et al. 1988).

However, recall Mellema (2001) who pointed out that because [WC] nuclei have i) generally much larger mass-loss rates compared to normal central stars, and ii) H deficient and metals enriched stellar winds, the cross-over to energy-driven nebulae is expected to arise for terminal velocities above $\sim$1000 km s^{-1} $> v_c$. Therefore PN with [WC] central stars are expected to have a long lasting momentum-driven phase which is known to be very sensitive to the non-linear thin-shell instability (Dwarkadas & Balick 1998).

But it seems very difficult to discuss in a quantitative way the present status of the nebula. For that we would need 1) a precise estimation of the mass-loss rates (AGB and post-AGB); 2) the temperature of the nebula. It seems that any quantitative discussion about these questions is almost impossible at this time.

Our results suggest that nebulae surrounding [WC] central stars are possibly related to a long-lasting momentum-driven phase, the turbulence being either triggered or more likely enhanced, by stellar wind inhomogeneities which appear ubiquitous for Wolf-Rayet nuclei, and are able to excite very effectively the non-linear thin-shell instability as well as other hydrodynamical instabilities.

The works of Garcia-Segura & Mac Low (1995) show that small-scale inhomogeneities affects the evolution of the interaction zone between the two winds: they excite the thin-shell instability. Dwarkadis & Balick (1998) also showed that a varying mass-loss rate with time implies the formation of more structures in the nebulae. It is not sure at all that wind clumps still affect the nebulae now. However, they surely affected the formation of the shell at the beginning of the interaction between the fast wind (which was possibly already clumped) with the previous slow wind. Wind clumps imply a varying mass-loss rate per se (with space and time); wind clumps are a very natural way to input small-scale perturbations. If the PN are indeed momentum-driven such perturbations are expected to last for a long time, giving ways to new perturbations exciting new instabilities (like Rayleigh-Taylor), maintaining energy injection for velocity-supported turbulence.

Additional effects can be considered, such as multipolar flows or orbital motion of binary nuclei. But these effects are believed to only affect the GLOBAL structure and dynamics of the nebulae. Turbulence requires small-scale instabilities. Given the high number (could be as high as 50 000; Lépine & Moffat 1999) of features which are present in (possibly) any [WC] stellar wind line-emission region, wind clumping may be an important factor. Stellar evolution scenarios of [WC] stars should certainly be influenced by stellar mass-loss rates being revised downwards.

5. Conclusions

We have presented the first extended study of velocity fields inside PN with [WC]-type nuclei. The analysis of a sample of 16 PN with emission-line nuclei is performed in comparison with 8 other nebulae. The following conclusions can be drawn.

– For the whole sample of PN, the median value of the expansion is about 25 km s^{-1}. The mean expansion velocities for [WC]-type nebulae are not significantly different from those of "normal" PN. For all types of PN, the expansion velocity is increasing with the nebular radius.

– All [WC]-type PN show evidence of strong (often supersonic) turbulent motions. Their velocity field is best represented by a turbulence superposed on an essentially constant expansion velocity. The non-[WC] PN show no evidence for turbulence, however the expansion velocity is found to increase outwards.

– No correlation is found between expansion or turbulent velocities and stellar parameters such as temperature, [WC]-subtypes and luminosity, or against terminal velocity of the wind, or nebular age.

– Finally, our results support the earlier suggestions that nebulae surrounding [WC] central stars are likely related to long-lasting momentum-driven phase bubbles. The detected turbulence could be either triggered, or enhanced, by stellar wind inhomogeneities that appear ubiquitous in Wolf-Rayet nuclei.

Acknowledgements. Many thanks to Coralie Neiner and Tony Moffat for valuable discussions. This project was partially supported by the CNRS in the frames of the JUMELAGE "Astronomie Pologne" programme. K. Gesicki acknowledges support from "Polish State Committee for Scientific Research" grant No. 2.P03D.020.17.

References

Acker, A., Ochsenbein, F., Stenholm, B., et al. 1992, Strasbourg – ESO Catalogue of Galactic Planetary Nebulae (ESO, Garching) (SECGPN)
Acker, A., Górny, S. K., & Cuisinier, F. 1996, A&A, 305, 944
Acker, A., & Grosdidier, Y. 2001, IAU Symp. 209 (Canberra), Wind Inhomogeneities in [WC] Central Stars: From Late- to Early-type Nuclei, in press
Acker, A., & Durand, S. 2001, IAU Symp. 209 (Canberra), An exhaustive study of [WC] central stars of PN, in press
Balick, B. 1994, Ap&SS, 216, 13
Bloecker, T. 1995, A&A, 299, 755
De Marco, O., Barlow, M. J., & Storey, P. J. 1997, MNRAS, 292, 86
Dwarkadas, V. V., & Balick, B. 1998, ApJ, 497, 267
Garcia-Segura, G., & Mac Low, M. 1995, ApJ, 455, 160
Gesicki, K., & Acker, A. 1996, Ap&SS, 238, 101
Gesicki, K., & Zijlstra, A. A. 2000, A&A, 358, 1058
Gesicki, K., Acker, A., & Szczerba, R. 1996, A&A, 309, 907
Gesicki, K., Zijlstra, A. A., Acker, A., & Szczerba, R. 1998, A&A, 329, 265

Górny, S. K. 2001, Ap&SS, 275, 67
Górny, S. K., & Stasińska, G. 1995, A&A, 303, 893
Goudis, C. D., Meaburn, J., & Whitehead, M. J. 1988, A&A, 191, 341
Grosdidier, Y., Acker, A., & Moffat, A. F. J. 2000, A&A, 364, 597
Grosdidier, Y., Acker, A., & Moffat, A. F. J. 2001a, A&A, 370, 513
Grosdidier, Y., García-Segura, G., Acker, A., & Moffat, A. F. J. 1999, in Proc. of the Observatoire de la Côte d'Azur, 1999 May 17–19 Meeting of the Radiative Transfer Group in Astrophysics (GRETA), Nice (France), ed. Ph. Stee, 199
Grosdidier, Y., Moffat, A. F. J., Blais-Ouellette, S., Joncas, G., & Acker, A. 2001b, ApJ, 562, 753
Kahn, F. D., & Breitschwerdt, D. 1990, MNRAS, 242, 505
Koeppen, J., Acker, A., & Stenholm, B. 1991, A&A, 248, 197
Kwok, S., Purton, C. R., & Fitzgerald, P. M. 1978, ApJ, 219, L125
Lépine, S., & Moffat, A. F. J. 1999, ApJ, 514, 909
McCarthy, J. K., Rich, R. M., Becker, S. R., et al. 1991, ApJ, 371, 380
Mellema, G., Raga, A. C., Canto, J., et al. 1998, A&A, 331, 335
Mellema, G. 2001, Ap&SS, 275, 147
Neiner, C., Acker, A., Gesicki, K., & Szczerba, R. 2000, A&A, 358, 321
Owocki, S. P., Runacres, M. C., & Cohen, D. H. 2000, ASP Conf. Ser. 204., ed. H. Lamers, & A. Sapar, 183
Peña, M., Stasińska, G., & Medina, S. 2001, A&A, 367, 983
Sahai, R., & Trauger, J. T. 1998, AJ, 116, 1357
Schwarz, H. E., Corradi, R. L. M., & Melnick, J. 1992, A&AS, 96, 23
Szczerba, R., Górny, S. K., Stasińska, G., Siodmiak, N., & Tylenda, R. 2001, Ap&SS, 275, 113
Tylenda, R., Acker, A., & Stenholm, B. 1993, A&AS, 102, 595
Zijlstra, A. A. 2001, Ap&SS, 275, 79